CONCRETE LIBRARY OF JSCE NO. 31, JUNE 1998

THE MECHANICAL BEHAVIOR OF COMPOSITE PRESTRESSED CONCRETE GIRDERS WITH CORRUGATED STEEL WEBS

(Translated from Concrete Research and Technology , Vol.8, No.1, pp.27-41, Jan.1997)

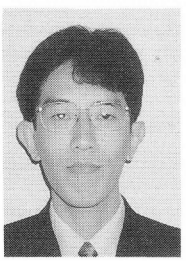

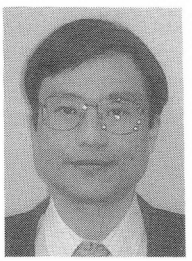

Kota YAMAGUCHI Takahiro YAMAGUCHI Shoji IKEDA

Flexural shear tests were conducted to clarify the mechanical behavior of steel girders with corrugated webs and composite prestressed concrete girders with corrugated steel webs. In this study, a new type of shear connection at the interface between the corrugated steel web and the lower concrete flange in the composite prestressed concrete girders was used, and also an application of composite prestressed concrete girders having corrugated steel webs to precast segmental construction is proposed. The experimental results indicate that girders with corrugated steel webs exhibit favorable shear resistance. Pure shear stresses are seen in the corrugated steel webs, indicated that prestressing forces are not transmitted to the corrugated steel web. A practical formula for estimating the buckling strength of corrugated steel webs, in which intermediate buckling mode is accounted for, is derived and good agreement is shown between the calculated values obtained by this formula and the experimental ones.

Keywords: corrugated steel web, prestressed concrete structures, composite structures, flexural shear behavior, shear buckling

---

Kota YAMAGUCHI is a civil engineer in the Structure Inspection and Analysis Section of the Structure Department of Pacific Consultants Corporation. He is a graduate of Yokohama National University and obtained his D.Eng. in 1996. He is a member of the JSCE, JCI, and JPCEA

Takahiro YAMAGUCHI is a research associate in Civil Engineering at Yokohama National University. He is a member of the JSCE, JCI, and JPCEA.

JSCE Fellow Shoji IKEDA is a professor of Civil Engineering at Yokohama National University. He served as president of the Japan Gas-Pressure Welding Association from 1989 to 1991 and as president of the Japan Prestressed Concrete Engineering Association from 1993 to 1995. He is a member of the IABSE, a fellow of the ACI, and a senior vice-president of the FIP. He specializes in the design and mechanics of reinforced concrete, prestressed concrete, and composite structures.

---

1. INTRODUCTION.

The advent of new construction methods in the field of prestressed concrete structures (PC structures) as external prestressing techniques have become established means there has a revolution in the development of composite structures; in France, in particular, girders have been developed using steel members for the web and concrete for the flange by the use of corrugated steel for the web and PC concrete for the composite structure [1][2]. Three bridges have already been built with composite structures, and in Japan there are two bridges using composite structures [3][4].

Steel plates can be formed into corrugated shapes on a metal-forming brake, and such corrugated steel plates are capable of withstanding large shear buckling strengths as a result of the corrugations. Since the transverse flexural stiffness of a corrugated steel web is negligible, and it has the advantage that prestressing forces are not dissipated unnecessarily in the steel web, and prestressing forces are transferred effectively to the concrete flange [2]. In recent years, the use of corrugated steel web for girders has been studied in France and Germany. In Japan, a study by Shimada in 1965 was the first foray into this field, and in 1974, Okamoto and Tagawa made exploratory studies on the use of corrugated steel plates for possible application in earthquake shear walls [5][6]. In 1975, there was an actual example of several kilometers of corrugated steel web being used as a crane girder at a factory [7]. However, the shear buckling characteristics of corrugated steel plates are still not fully understood, especially as regards intermediate buckling and post-buckling strength, with the result that no method of calculating shear buckling strength has been standardized as yet. Especially, studies concerned with corrugated steel webs for composite PC girders have newly been introduced, and for the most part of studies have been made into the flexural behavior of the composite PC girders with corrugated steel web, with the result that their flexural shear behavior are not known well at the present time.

In this study, flexural shear tests were conducted on girders with corrugated webs together with composite PC girders using corrugated steel webs. The shear buckling strength of the corrugated steel plates and flexural shear behavior of the steel girders containing the corrugated webs were investigated, together with composite PC girders using corrugated webs. A formula for estimating the shear buckling strength of corrugated steel plates, taking into account the intermediate buckling mode, is proposed. Close attention is paid to the interface between the steel girder and the concrete flange, and a new type of shear connection is proposed. Finally, an application of composite PC girders with corrugated webs to precast segmental construction is proposed.

2. DESCRIPTION OF SPECIMENS AND LOADING TEST

The loading tests were conducted in three stages: a) the shear buckling behavior of the corrugated steel plates (SB Series); b) an examination of the flexural shear characteristics of the corrugated steel webs (ST Series); and c) the flexural shear characteristics of composite PC girders with

Table 1. List of Specimens

(a) SB Series

Specimen	Web Thickness t_w [mm]	$h^{1)}/t_w$	Web Material	Corrugation Height [mm]
SB-C-16	1.6	469	SPHC	60
SB-C-32A, B	2.2	434	SS400	
SS-C-5	5.0	150		
SS-C-6	6.0	125		

NOTES: 1) h : clear distance between flanges

(b) ST Series

Specimen	Web Thickness t_w [mm]	$h^{1)}/t_w$	Web Material	Corrugation Height [mm]
ST-PL-23	2.3	135	SPHC	0
ST-PL-4	4.0	78	SS400	
ST-C-23	2.3	135	SPHC	40
ST-C-4	4.0	78	SS400	

NOTES: 1) h : clear distance between flanges

(c) PC Series

Specimen	Prestress Level [MPa]		Web Thickness t_w [mm]	$h^{1)}/t_w$	Corrugation Height [mm]	Connection Method [2)]
	PC Tendon	Extreme Fiber Stress on Tension Side				
PL-23	$0.6f_{py}$	6.8	2.3	135	0	Stud
C-23		7.2			40	
C-4		7.2	4.0	78		
C-23-Pcc		10.4	2.3	135		
C-4-ENC		7.0	4.0	70		Embed [3)]
C-4-REB		6.5				Deformed Rebar

NOTES: 1) h : clear distance between flanges
2) Interaction of steel web to top concrete flange by studs
3) Connection of web to bottom concrete flange by direct embedding

Specimen nomenclature:
PL : Common steel web, C : Corrugated web, 16 : Web thickness 1.6mm, 23 : Web thickness 2.3mm, 32 : Web thickness 3.2mm, 4 : Web thickness 4.0mm, 5 : Web thickness 5.0mm, 6 : Web thickness 6.0mm.
Pcc : precast structure with corrugated steel web where the steel girder portion has non-continuous steel flange; ENC : web is embedded into the bottom concrete flange; REB : web with deformed steel rebar welded at the lower edge and embedded into the bottom concrete flange as a shear-resisting device.

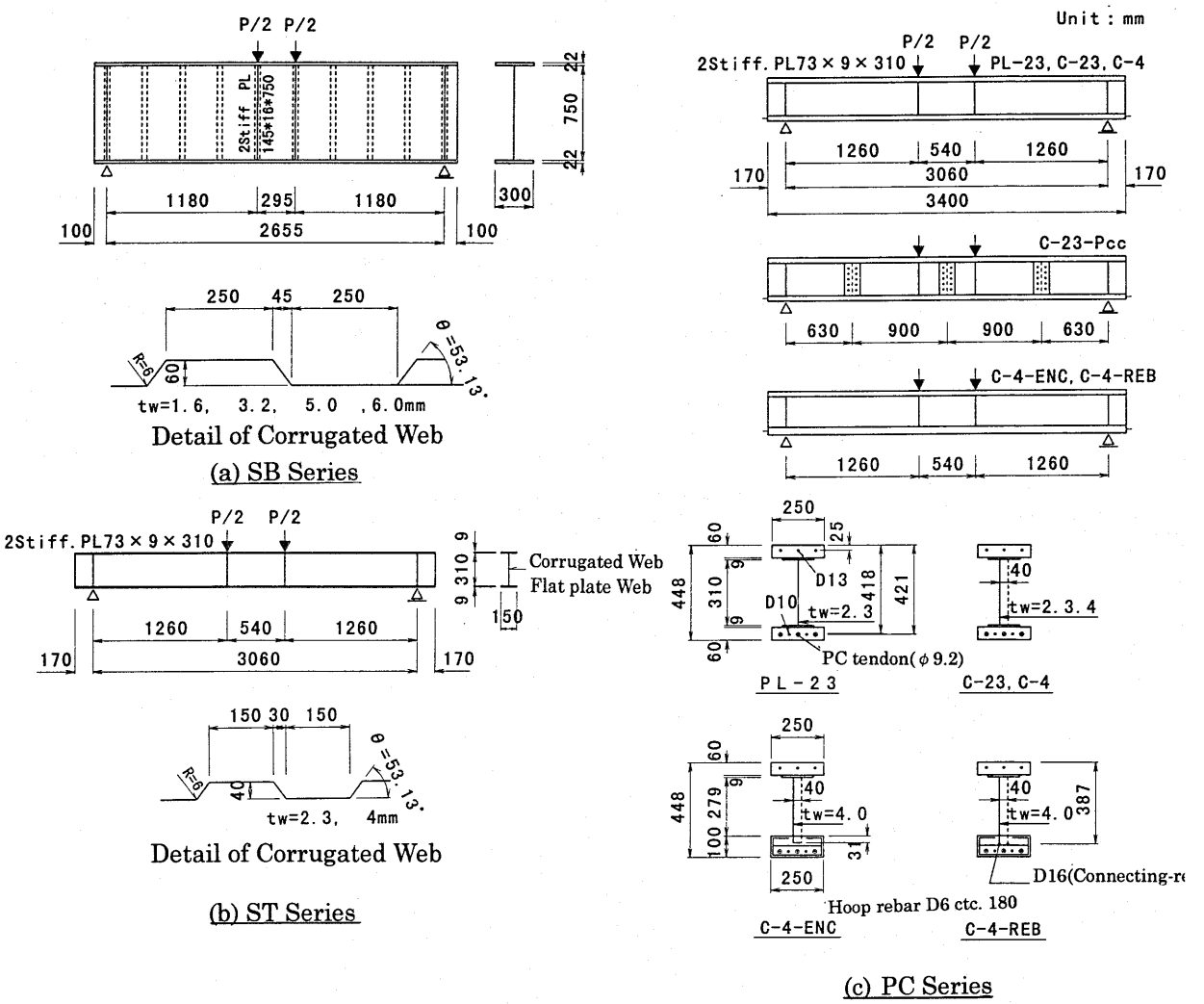

Fig. 1. Details of Specimens

corrugated steel webs (PC Series) [8][9][10][11]. The specimens used for the loading tests consisted of a total of 14 specimens, and these were fabricated with I-sections. The characteristics of the specimens used for the loading tests and their physical details are shown in Table 1 and Fig. 1.

The SB Series tests were conducted in order to investigate the shear buckling strength of the corrugated steel plates themselves and the post-buckling strength of girders using the corrugated steel webs. The girder specimen had an a/d (shear span length/beam height) of 1.4, and had a symmetrical I-section. The test parameters included web thickness, with four web thickness as 1.6 mm, 3.2 mm, 5.0 mm, and 6.0 mm. The specimens were designed so that each rectangular panel would buckle between two folds of the corrugated plates. As regards the mechanical properties of the steel plates used in the specimens, specimen SB-C-16 was designed for elastic buckling, specimen SB-C-32A for inelastic buckling, and specimens SB-C-5 and SB-C-6 for plastic buckling.

Specimen SB-C-32B was used to investigate the effect of a longitudinal stiffener, and is used after the loading test for specimen SB-C-32A by shifting the load and support point to determine the effect on the girder when there is no vertical stiffeners in the specimen.

The ST Series tests were conducted in order to investigate the flexural shear behavior of steel girders with corrugated webs, and the specimens are of the same shape as the PC Series steel girders. The specimen had an a/d of 3.8, and a symmetrical I-section. The test parameters included type of web and web thickness; webs were of two types, one without corrugations (a flat steel web) and the other of corrugated type. Web thickness was of two values: 2.3 mm and 4.0 mm. Specimens ST-PL-23 and ST-PL-4 used flat steel plates for their webs, and were desined for comparison of the flexural shear behavior of the flat steel web with the corrugated web. Also, specimens ST-C-23 and ST-C-4 had corrugated steel plates as their webs to investigate the differences in the flexural shear behavior with varying web thickness.

The PC Series tests were conducted in order to investigate the flexural shear behavior of composite PC girders with corrugated steel webs, and the steel girders were of the same shape as the ST Series specimens described above. Specimen PL-23 had flat steel plates as webs, and was used to compare the flexural shear behavior of a flat steel plate web with the corrugated steel web. Specimen C-23 was designed so that shear buckling of the corrugated web would occur first. Specimen C-4 was designed with a web thickness of 4.0 mm so that the corrugated would not buckle under shear; it was also designed so that failure would occur due to the PC tendons yielding. Specimen C-23-Pcc was investigated as a possible design for a composite PC girder with a corrugated web with the intent of studying possible application to precast segment structures, and was a girder with a divided corrugated steel web. Furthermore, with this specimen, a 10 mm open space was made in the steel flange between each divided steel girder to create a discontinuity in the flange. The web was secured with high-tension bolts using a friction connection. Specimen C-4-ENC was a composite PC girder with a corrugated steel web. It has been given further attention at the interface of the steel girder and the concrete flange, and the corrugated steel web is embedded into the lower concrete flange. Specimen C-4-REB had a new type of shear connection at the interface between the corrugated steel web and the lower concrete flange in the composite PC girders as proposed by the authors. This new shear connection consists of a deformed reinforcing bar (connecting rebars) welded continuously in the longitudinal direction at the lower end of the corrugated web at the crest of a corrugation, and this embedded in the lower concrete. To integrate the upper steel and upper concrete flanges in all specimens, stud connectors were used. With the exception of specimens C-4-ENC and C-4-REB, the lower steel flange and the lower concrete flange were integrated with studs, with the studs welded at 50 mm spacing along its length, perpendicular at every 100 mm (to the web).

In applying loads to the specimens, there were supported simply as shown in Fig. 1. The load was applied at two static points in the middle of the span. For only specimen SB-C-32B of the SB Series, the left side shear span was 850 mm with the static load applied at a concentrated point. In

Table 2. Mechanical Properties of Steel Components

Type and Size		Application	Yield Strength σ_y (MPa)	Tensile Strength σ_u (MPa)	Young's Modulus E (GPa)
SD295A	D 61 [1)]	Hoop	330	550	200
	D10 [1)]	Tension bar	370	530	200
	D13 [1)]	Compression bar	360	540	190
	D16 [1)]	Connection bar	430	630	190
SPHC	1.6 mm	Web	260	370	200
	2.3 mm		480	780	200
SS400	3.2 mm		320	480	200
	4.0mm		380	460	210
	5.0mm		340	460	210
	6.0mm		320	450	210
	9.0mm	Flange	310	460	210
	16.0mm	Stiffener	260	440	210
	22.0mm	Flange	260	420	210
SBPR 1080/1230,9.2ϕ		PC Tendon	1260	1290	190
MFL 6ϕ x 40 [2)]		Stud	360	480	---

Note: 1)Size is expressed in terms of JIS ; D means "Deformed" and the number is the nominal diameter
2)Milsheet value.

Table 3. Concrete Strengths

	Compressive Strength f'_{ck} (MPa)	Tensile Strength σ_t (MPa)	Young's Modulus E (GPa)
Upper Concrete Flange	50	3.8	27
Lower Concrete Flange	48	3.6	28
Grout	44	-	-

other specimens, the load was applied in the static manner, and the force was introduced until the yield load P_y or the buckling load P_B. (Where P_y is the load at which the tensile strain of the main steel member reaches its yield value and P_B is the load at which shear buckling occurs in the steel web.) The displacement control method was used until the specimen failed. The Measurements of deflection were taken at the center of each span, the loading point, and at the center of the shear span. Measurements of strain were taken at the middle of the span and at the center of the shear span.

The mechanical properties of the steel components of the test specimens are shown in Table 2. The strengths of the concrete materials for the PC Series are shown in Table 3.

3. EQUATION FOR CALCULATING SHEAR BUCKLING STRENGTH

A corrugated steel web does not resist a bending moment, and it is known that it can resist only shear stresses [2]. For this study, consider a fixed supported rectangular plate subjected to the action of shearing forces uniformly distributed along the edges, as shown in Fig. 2 [12]. The buckling modes of the trapezoidal-form corrugated steel plate consist of a local buckling corresponding to a partial panel buckling, a general buckling corresponding to overall panel

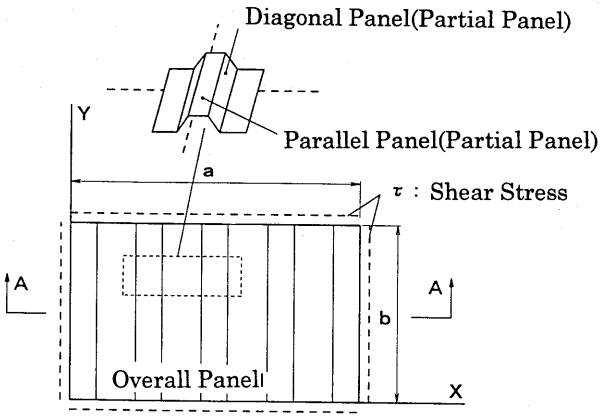

(a) Coordinate system

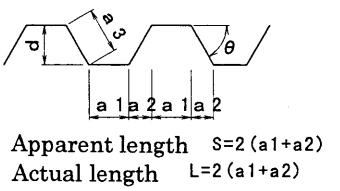

(b) Cross-section

Fig. 2 Corrugated Steel Plate

buckling, and intermediate buckling corresponding to a combination by linking of the first two modes. In this study, a formula for estimating the buckling strength of corrugated steel plate taking into account these three types of buckling, is proposed [11].

In the case of the local buckling mode, the shear buckling formula can be derived as Eq.(1):

$$\tau_{cre,L} = \frac{\pi^2 E}{12\left(1-\nu^2\right)}\left(\frac{t_w}{b}\right)K_s \qquad (1)$$

$$K_s = 5.6 + \frac{8.98}{\alpha^2} \qquad \alpha \le 1$$

$$K_s = 8.98 + \frac{5.6}{\alpha^2} \qquad \alpha \ge 1$$

$\alpha = a/b$ a : maximum length of partial panel (a_1 or a_3).

where:

$\tau_{cre,L}$: elastic local buckling strength
a : partial panel length
b : web height
t_w : web thickness
E : Young's modulus
ν : Poisson's ratio
α : aspect ratio of partial panel
K_S : plate buckling coefficient (fixed support).

In the case of the general buckling mode, a shear buckling formula was derived by J.T. Easley for a corrugated metal shear diaphragm as a model for an orthotropic panel. This will be used here and is given as Eq. (2) [14].

$$\tau_{cre,G} = 36\beta \frac{(EI_Y)^{1/4}(EI_X)^{3/4}}{b^2 t} \tag{2}$$

where:

$\tau_{cre,G}$: elastic general buckling strength
I_y : moment of inertia per unit length of Y-axis
I_x : moment of inertia per unit length of X-axis
β : buckling formula coefficient (fixed support : $\beta = 1.9$)

Next, material non-linearity is taken into account by introducing a plate slenderness parameter, λ_s. In the local buckling and general buckling modes, the elastic buckling strengths are given by Eq.(1) and Eq.(2), respectively. Also, shear buckling strength in consideration of the material non-linearity are given in Eq.(3.1) ~Eq.(3.3) by using plate slenderness parameter λ_s. In this study, the buckling curves given by FHWA curves, which disregard the strain hardening, are used, and the curves in the inelastic region are made straight-lines [13][15].

$$\tau_{cr}'/\tau_y = 1 \qquad : \lambda \le 0.6 \tag{3.1}$$

$$= 1 + 0.614(0.6 - \lambda_s) \qquad : 0.6 \prec \lambda_s \le \sqrt{2} \tag{3.2}$$

$$= 1/\lambda_s^2 \qquad : \lambda_s \succ \sqrt{2} \tag{3.3}$$

where:

λ_s : plate slenderness parameter ($\sqrt{\tau_y/\tau_{cre}}$)
τ_Y : shear yield strength
τ_{cre} : elastic shear bucking strength
($\tau_{cre,L}$: local elastic buckling strength,
$\tau_{cre,G}$:general elastic buckling strength)
τ_{cr}' : shear buckling strength in consideration of material non-linearity
($\tau_{cr,L}'$: local shear buckling strength in consideration of material non-linearity,
$\tau_{cr,G}'$: general shear buckling strength in consideration of material non-linearity)

The intermediate buckling mode consists of an interaction between local buckling and general buckling, and the formula for the shear buckling strength can be described by combining the local buckling strength and the general buckling strength. In this study, the focus is on agreement between the two stresses, and the correlation between the two has been considered. The case of $m = n = 4$ is chosen for this study, and is described as Eq.(4) as follows.

$$\left[\frac{\tau_{cr}}{\tau_{cr',L}}\right]^m + \left[\frac{\tau_{cr}}{\tau_{cr',G}}\right]^n = 1 \qquad (4)$$

where:

τ_{cr} : shear buckling stress of corrugated web panel

m,n : coefficient of interaction between local buckling and general buckling
(In this study, the case of m = n = 4 is chosen.)

In using the $m = n = 4$ relationship, the shear buckling strength τ_{cr} can be derived as Eq. (5) as follows.

$$\tau_{cr} = \tau_{cr',L} \sqrt[4]{\frac{1}{1+\left[\frac{\tau_{cr',L}}{\tau_{cr',G}}\right]^4}} \qquad (5)$$

The correlation between local buckling and general buckling in Eq. (5) is shown in Fig. 3. Correlation is the strongest when the values of both local and general buckling stress approach each other. When the difference between local buckling and general buckling increses, the correlation grows weaker and, from the relationship given in Eq. (5), the shear buckling stress can be calculated from the local buckling stress and the general buckling stress. Hence, the shear buckling stress for corrugated web τ_{cr} obtained with Eq. (3.1) ~ Eq.(3.3) will enable the local buckling stress $\tau_{cr',L}$ and the general buckling stress $\tau_{cr',G}$ to be calculated by substituting values into Eq.(5) .

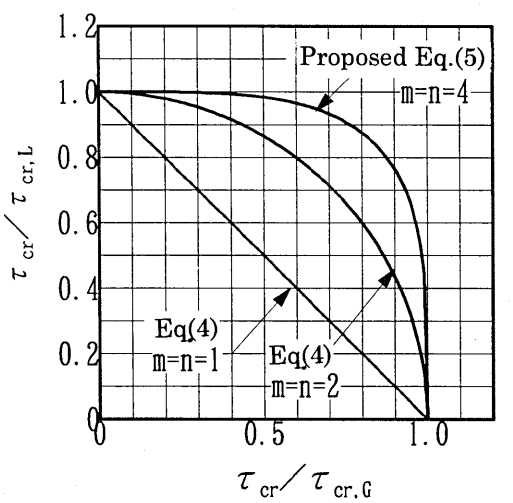

Fig. 3 Relationship between Local Buckling and General Buckling

4. FLXURAL ANALYSIS OF LOAD-CARRING CAPACITY AND DEFLECTION

In order to analyze the load-carrying capacity and deflection of girders with corrugated webs, a fiber model in which the cross section is replaced by many fiber elements is used to carry out calculations.

In this analysis of the girder, the following five basic assumptions were made:

1) Cross sections of the girder remain plane (the Bernoulli-Eulers assumption)
2) The shear deformation of the steel web is considered
3) The loss of shear rigidity of the corrugated steel web is treated as a loss of cross-sectional area of the steel plate, and this loss of cross-sectional area is considered on the effective cross sectional area depending on the ratio of apparent length S to actual length L as Eq.(6) [7].

$$A_w^e = A_w \cdot S / L \qquad (6)$$

Where:

A_w^e : effective cross-sectional area of the web
A_w : actual web cross-sectional area
S : apparent length
L : actual length

4) For the PC Series, a normal strain in excess of 5 000μ at the extreme fiber of the upper concrete flange is considered the ultimate stage
5) For the PC Series, the steel girder and the concrete flange interact fully

Fig.4 shows the stress–stress relation concrete and steel materials used in the calculation. Furthermore, longitudinal rigidity was set at null so that the corrugated web did not resist any bending moment.

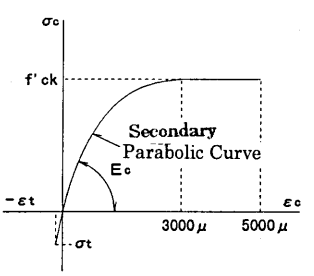

f'ck=50MPa, σt =3.8MPa.
εt =135μ, Ec =27GPa

(a) Concrete

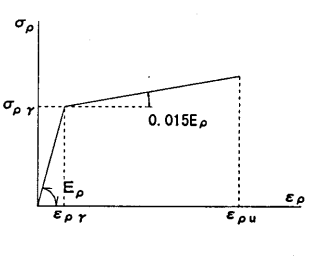

σpy =1260MPa, εpy =σpy /Ep .
εpu =50000μ, Ep =190GPa

(b) PC tendon

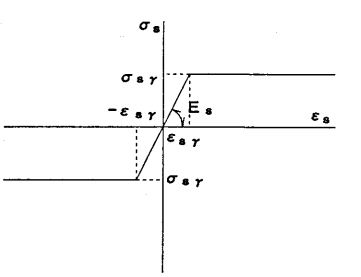

σy : Yield Strength.
εy : Yield Strain

(c) Reinforcement and Steel Plate

Fig. 4. Stress-Strain Relation of Materials

5. EXPERIMENTAL RESULTS AND DISCUSSIONS

5.1 THE SB SERIES

5.1.1 SHEAR BUCKLING STRENGTH OF CORRUGATED STEEL PLATES

Table 4 gives calculated values and experimental results for the SB Series. The calculated shear buckling loads $P_{sb,L}$ and $P_{sb,G}$ are the local buckling load and general buckling load, respectively, developed in consideration of material non linearity. The Intermediate Buckling I in the $m = n = 2$ case (Column ③ of table 4), is the calculated value given by Eq.(4) [16]. The Intermediate Buckling II in the $m = n = 4$ case, (Column ④ of table 4), is the calculated value given by Eq.(5). The measured shear buckling load P_{sbt} is the value recorded prior to the buckling which occurred first and the loss of its strength.

The buckling mode of specimens SB-C-16, SB-C-32, and SB-C-5 was local buckling where parallel panels of the rectangular panel buckled between the two folds in the corrugation, and for specimen SB-C-6 was intermediate buckling where, with the exception of the end panel, the remaining partial panels buckled simultaneously.

The calculated shear buckling load and the experimental results will be discussed in terms of the differences in buckling mode among specimens.

The calculated value for local buckling load in Column ① of Table 4 shows good agreement with the experimental results, but for specimen SB-C-6, which suffered intermediate buckling, the calculated values in Column ① and Column ② are larger by 17% than the measured values. Also, in Column ③ for Intermediate Buckling I in the $m = n = 2$ case, the calculated value for Specimen SB-C-6 is smaller by 17% than the measured value. However, in Column ④ for Intermediate Buckling II in $m = n = 4$ case, the calculated value for Specimen SB-C-6 is in close agreement with the measured value. On the other hand, for the SB Series, calculated values for Intermediate Buckling I are smaller by 20% than the measured values, but for Intermediate Buckling II the differences are smaller than 10%. Thus, regardless of the buckling mode, and it is confirmed that calculated results can be expected to be quite accurate.

The experimental results for the SB Series, together with the existing experimental results by Lindner, et al. and Hanada, et al. are given in Fig.5 along with calculated values given by the proposed shear buckling formula [16][17]. Calculated values and test results are in close agreement, and the correlation coefficient and variance are 0.94 and 9.5%, respectively. The arithmetic mean of the ratio of experimental result to calculated value is 1.010. Hence, the proposal in Chapter 3 for calculating shear buckling is able to evaluate the experimental results with fair accuracy. Further, not only the shear buckling strength, but also the buckling mode of the corrugated steel plate can be evaluated uniformly. When the corrugated steel plate buckles under

Table 4. Shear Buckling Load

(Unit: kN)

Specimen	Calculated Value				Measured Value	Measured Value / Calculated Value				Buckling Mode
	Local Buckling $P_{sb,L}$ ①	General Buckling $P_{sb,G}$ ②	Intermediate Buckling I ③	Intermediate Buckling II ④	P_{sbt} ⑤	⑤/① ⑥	⑤/② ⑦	⑤/③ ⑧	⑤/④ ⑨	
SB-C-16	152.7	349.4	139.9	151.3	165.8	1.09	0.47	1.19	1.09	Local
SB-C-32A	757.6	856.8	567.6	672.4	816.2	1.08	0.95	1.44	1.21	Local
SB-C-5	1 398.6	1 398.6	989.0	1 176.1	1 311.6	0.94	0.94	1.33	1.12	Local
SB-C-6	1 597.4	1 597.4	1 129.5	1 343.2	1 362.6	0.85	0.85	1.21	1.01	Linked

$P_{sb,L}$: local buckling load, $P_{sb,G}$: general buckling load, P_{sbt} : buckling load (measured value)
Intermediate Buckling I : calculated value from Eq.(4) when m = n = 2
Intermediate Buckling II: calculated value from Eq.(5)

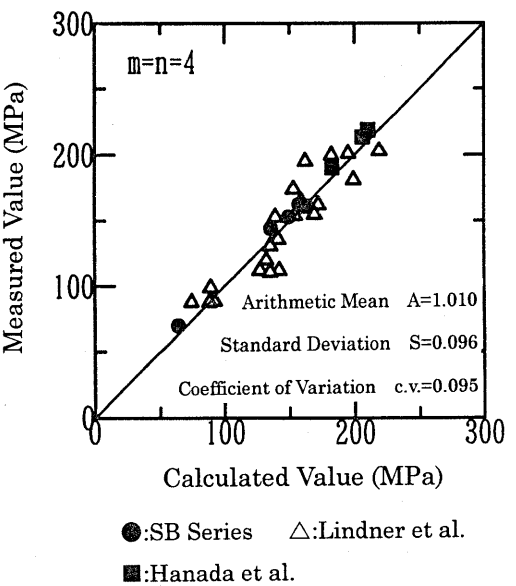

Fig. 5. Shear Buckling Strength

intermediate buckling mode, it has been shown that the buckling stress is a maximum of about 15% lower than the local buckling stress and general buckling stress.

5.1.2 POST-BUCKLING STRENGTH OF GIRDERS WITH CORRUGATED WEBS

The relationship between load and vertical deflection at the center of the span are given in Fig. 6 and Fig. 7 for the SB Series. The buckling process of specimen SB-C-16 is shown in Photo. 1.

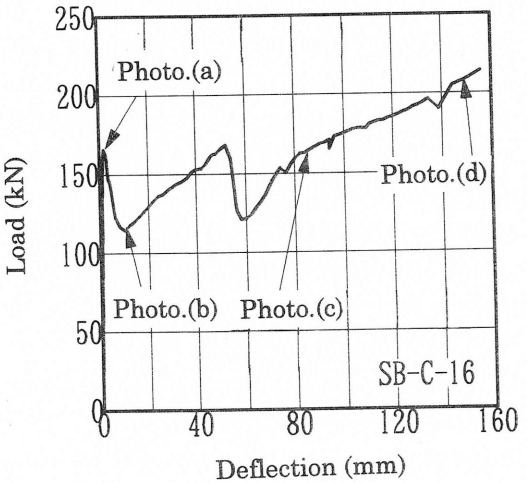

Fig. 6. Load-Deflection Relationship (SB-C-16)

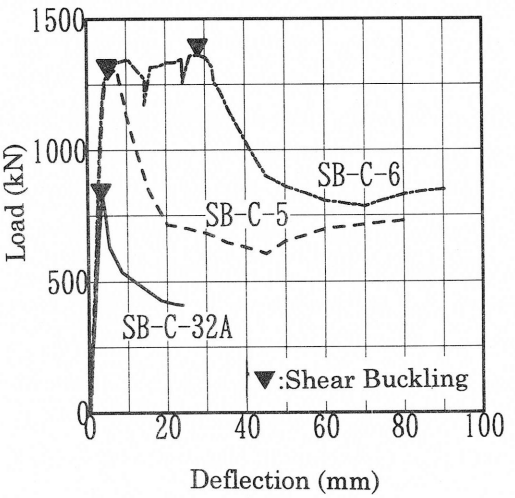

Fig. 7. Load-Deflection Relationship (SB-C-32A).

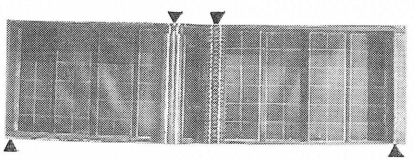

(a) First web buckling occurs in rectangular panel of corrugated steel web at the left half span of girder (δ =1.5mm)

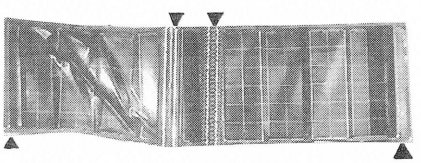

(b) Out-of-plane deformation of the web plate grows at the left half span of girder (δ =10mm)

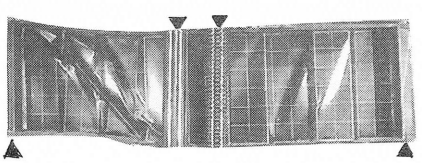

(c) Successively, web buckling occurs at the right half span of girder (δ =52mm)

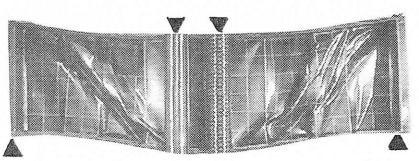

(d) Showing well-developed tension field (δ =100mm)

Photo. 1 The Buckling Process (SB-C-16)

For girders with a corrugated web, once the web buckles, the diagonal panel becomes twisted and deforms out of the plane. The cross section of the web changes greatly in shape, and the web loses its strength, so the load-carrying mechanism is completely different from that of normal plate girders[11]. With the exception of Specimen SB-C-32A for girders with corrugated webs, which had a deflection of 22 mm when loading was terminated, the specimens recovered their load-carrying capacity from the minimum stable loading condition, and indicated that the tension field

was created in the buckled web panel. In Specimen SB-C-16, when the load-carrying capacity was recovering from the first buckling load, the shear span --which till then had not exhibited any signs of shear buckling-- buckled. It was confirmed that the vertical displacement increased while at the same time a tension filed appeared, and its load-carrying capacity increased beyond the buckling load. In specimen SB-C-16, the collapse load was 208 kN, which was 1.25 times larger than the shear buckling load. The calculated value of post-buckling load was 201kN, which corresponds with the value given by the modified Baslers theory as proposed by Fujii, while the measured value was about 1.03 times lager than Fujii's calculated value [15][18][19]. It has thus been confirmed that for girders with corrugated webs that if the structural framework created by the flanges and longitudinal stiffeners is adequate, then the post-buckling strength is the same as for normal plate girders. However, since the longitudinal stiffener is usually eliminated in the girders with corrugated webs, a sufficient tension field with a sturdy framework cannot be relied on, and there will be a rapid loss of strength with buckling. Thus it is not wise to depend on post-buckling strength.

5.1.3 THE LOAD CONCENTRATION POINT

In the case where there is no longitudinal stiffener at the supports and at the loading point, the relationship between load and vertical deflection at the loading point is shown in Fig. 8 for Specimen SB-C-32B. At a point under the load concentration point, local buckling occurred over about one-half of a corrugation in the web. The load at which local buckling occurred was about 20% less than the shear buckling load calculated form the shear buckling strength formula proposed in Chapter 3. It is known that bearing stress of girders with corrugated webs is distributed two corrugations, and in the case of Specimen SB-C-32B the concentrated load was applied partially on one panel which caused local yielding in the web [7]. For this reason it is considered best to spread the load over more than one corrugation at points where loads will be concentrated. Also, in Specimens SB-C-16, SB-C-32A, SB-C-5, and SB-C-6, shear buckling occurred in partial

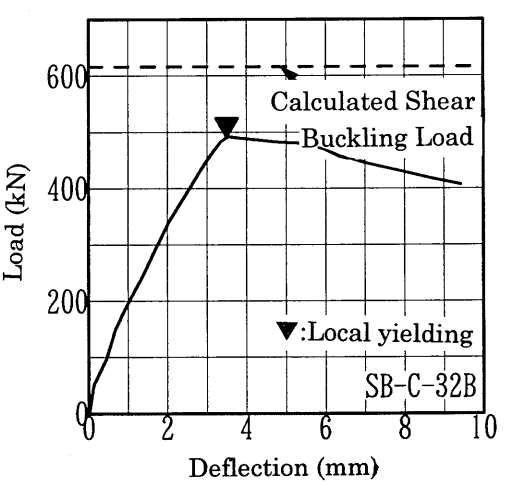

Fig. 8. Load-Deflection Relationship

panels, corrugated webs are expected to be lager out-of-plane rigidity, it has been confirmed that the longitudinal stiffener can be eliminated in areas away from support points where loads will be concentrated.

5.2 THE ST SERIES

5.2.1 STUDIES OF LOAD-CARRYING CAPACITY

The experimental results and calculated value for the ST Series are shown in Table.5. The yield load P_y and ultimate load P_u are calculated values obtained through fiber model analysis. The yield load P_y, P_y is the calculated value at which the extreme fiber stress of the flange reaches its yield value. The ultimate load P_u, P_u is the calculated value at which full plasticity occurs at certain critical sections of a girder. The shear buckling load P_{sb}, P_{sb} is the calculated value given in the shear buckling formula described in Chapter 3. The yield load P_{yt} ,P_{yt} is the measured value when the extreme fiber strain reaches its yield value, and the ultimate load P_{ut}, P_{ut} is the measured value when plastic local buckling occurs in the middle of the upper flange. The shear buckling load P_{sbt}, P_{sbt} is the measured value first confirmed by observation when the shear buckling occurs in the web.

In the case of specimen ST-PL-23, the yield load and ultimate load are disparity between the calculated values and measured values due to the shear buckling in the web. The yield load of all specimens with the exception of ST-PL-23 there is some variance between the calculated and measured values due to non-linear phenomena influencing the loading test. For the ultimate load, the calculated values and the measured values are in good agreement because the cross sections of the specimens are fully plastic

The relationship between load and vertical deflection at the loading point for the ST Series is shown in Fig. 9. For specimens ST-C-23 and ST-C-4, the load-deflection relationship is in good agreement from the initial stage to the final stage of loading test, and indicating that the web thickness had very little effect on girders with corrugated webs. For specimen ST-C-4, the corrugated steel plate was unable to resist the bending moment, and flexural rigidity was 22% less than for specimen ST-PL-4. The ultimate load was smaller by about 15%. In addition, shear buckling in the web occurred only in Specimen ST-PL-23, and did not occur in the web of the other three specimens. In the ultimate limit state for the ST Series, local plastic buckling occurred in the upper flange in the middle of the span.

5.2.2 STRESS DISTRIBUTION OF CORRUGATED STEEL WEB

The normal stress distribution at the center of the span for specimen ST-C-23 is shown in Fig. 10. The measured value is affected by the bending moment near the connection between web and flange, and some normal stress is developed. However, at some distance from the joint, normal stress is not observed in the web, and it is confirmed that the corrugated steel web is unable to

Table 5. Load Test of Girders with Corrugated Steel Webs

(Unit: kN)

Specimen	Calculated Value			Measured Value			Measured Value / Calculated Value		
	P_y ①	P_u ②	P_{sb} ③	P_{yt} ④	P_{ut} ⑤	P_{sbt} ⑥	Yield Load ④/①	Ultimate Load ⑤/②	Buckling Load ⑥/③
ST-PL-23	236.7	254.4	116.7	186.3	187.2	117.7	0.79	0.74	1.01
ST-PL-4	246.7	256.2	419.0	211.3	250.5	---	0.86	0.98	---
ST-C-23	216.2	216.2	323.4	187.2	205.2	---	0.87	0.95	---
ST-C-4	216.2	216.2	519.6	181.7	212.8	---	0.84	0.98	---

P_y : yield load, P_u : ultimate load, P_{sb} : shear buckling load, subscript t denotes measured value

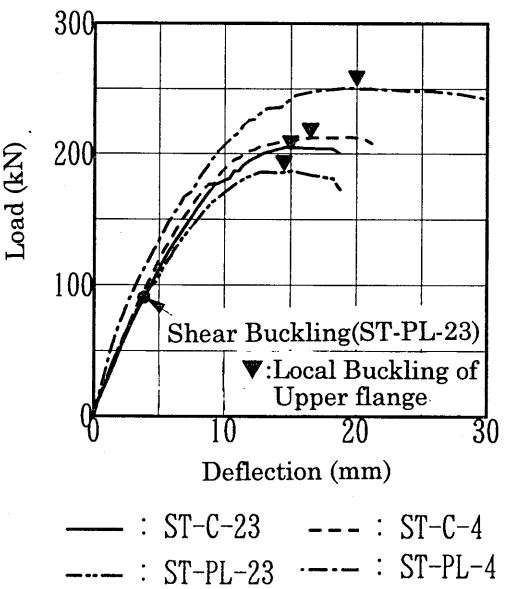

Fig. 9. Load – Deflection Relation of Test Specimens

resist the bending moment. At extreme fiber of the upper flange and the lower flange, the normal stress calculated by beam theory, that considered the longitudinal rigidity of the corrugated web to be null, is in good agreement with the measured value. Next, the shear stress distribution in the corrugated steel web is shown in Fig. 11 for Specimen ST-C-23. Cal-I is the shear stress obtained by beam theory, and Cal-II is the mean shear stress obtained by calculation. The measured value is obtained from triaxial gauge readings taken on the web plate at the center of the shear span. The measured value of shear stress in the web is distributed uniformly in the direction of web height, since the web gives no resistance to the bending moment, and it is confirmed that the mean shear stress is in good agreement with the Cal-II calculated value.

The distributions of shear stress in the parallel panel and the diagonal panel are shown in Fig. 12 for Specimen ST-C-23. The maximum principal stress, minimum principal stress, and maximum

shear stress for both parallel and diagonal panels should be about the same, and it is confirmed that they should become a pure shear stress field. It has become clear that in both parallel and diagonal panels that the pure shear stress field are of about the same, and that the entire corrugated steel web forms a uniform pure shear stress field.

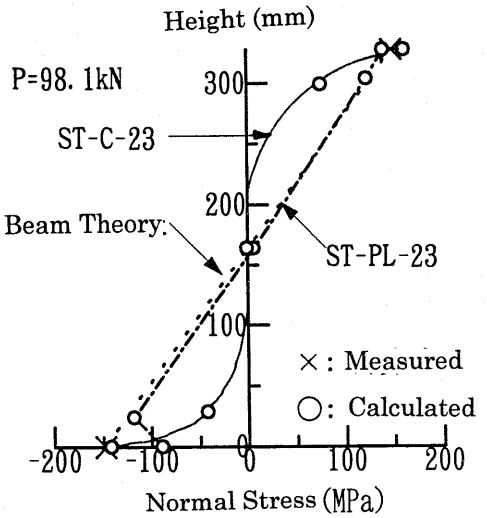

Fig. 10. Distribution of Normal Stress

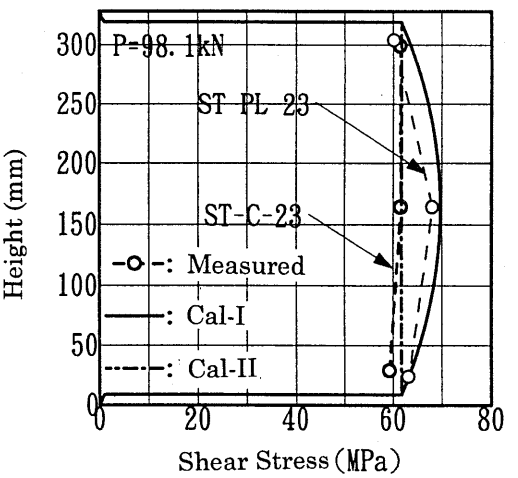

Fig. 11. Distribution of Shear Stress

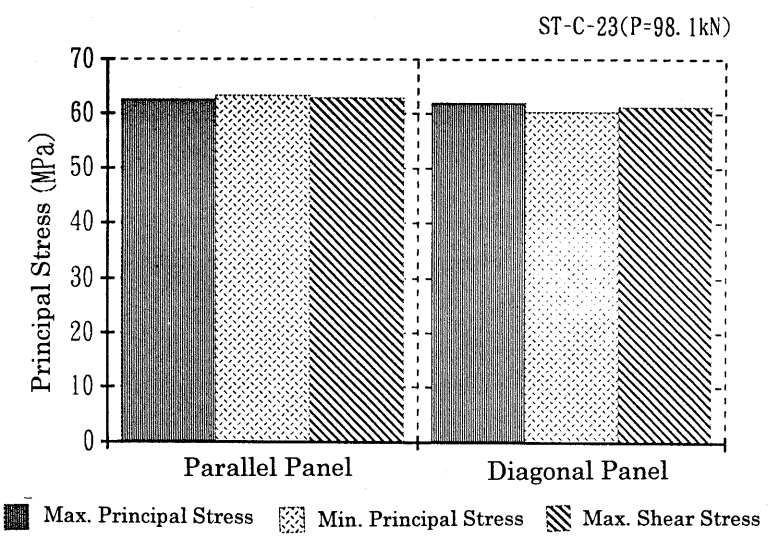

Fig. 12. Stress Distribution of Corrugated Steel Web

5.3 THE PC SERIES.

5.3.1 STUDIES OF LOAD CARRYING CAPACITY

The experimental results and calculated values for the PC Series are shown in Table 6. The cracking load P_{cr}, yield load P_y , and ultimate load P_u were calculated using the fiber model analysis. P_y is the yield load at which the stress of the PC tendon reaches its yield value. P_u is the ultimate load at which the extreme fiber strain at the top concrete flange reaches its ultimate strain. P_{sb} is the shear buckling load given by the shear buckling formula described in Chapter 3. Also, the cracking load P_{crt}, P_{crt} is the measured value first confirmed by observation when the flexural crack occur in the lower concrete flange. The yield load P_{yt}, P_{yt} is the measured value at which the stress of the PC tendon reaches its yield value. The ultimate load P_{ut} , P_{ut} is the measured value equivalent to the maximum applied load in the loading test. The shear buckling load P_{sbt} is the measured value when out-of-plane twisting was first observed.

In the case of specimen PL-23, due to shear buckling of the web, there was a difference between calculated value and measured value of load carrying capacity which was related to the yield load and ultimate load. With the exception of specimen PL-23, the effects of drying shrinkage meant that the measured cracking load was 30% smaller than the calculated value. Also, for the yield load, ultimate load, and shear buckling load, the calculated values and measured values were in close agreement with each other.

The relationships between load and vertical deflection at the center of the span for specimens PL-23, C-23, and C-4 are shown in Fig. 13. For the PC Series, the cross-sectional stiffness is larger than in the case of the ST Series, so the concrete for the flange, and the ultimate strength of the girder is improved. As shown in Photo.2, local buckling occurred in a parallel panel. For specimen C-23, similar to the SB Series, the shear buckling load became the bifurcation values. Later, the load-carrying capacity fell gradually, and it is confirmed that the post-buckling behavior of this specimen is quite different from that of specimen PL-23 in which the normal steel web experienced shear buckling. The shear buckling load for specimen C-23 with a corrugated steel web is more than three times greater than that of specimen PL-23 which has a normal steel web, and it is quite apparent that the use of the corrugated web improves shear buckling strength. The ultimate stage in the case of specimen PL-23 consisted of failure in the upper concrete flange at the end of the girder, while cracks were also seen in the upper concrete flange between the end of the girder and the center of the shear span for specimens PL-23 and C-23 due to shear buckling in the web. In the load-deflection relationships for specimens C-23 and C-4, until buckling of the web in specimen C-23 occurs, the curves for the two are almost the same. Although the thickness of the corrugated webs differed, the flexural shear behavior of these composite PC girders with corrugated webs was not affected.

Table. 6 Load Test of Composite PC Girder with Corrugated Wed

(Unit: kN)

Specimen	Calculated Value				Measured Value				Measured Value / Calculated Value			
	P_{cr} ①	P_y ②	P_u ③	P_{ab} ④	P_{crt} ⑤	P_{yt} ⑥	P_{ut} ⑦	P_{sbt} ⑧	Cracking ⑤/①	Yield ⑥/②	Ultimate ⑦/③	Share Buckling ⑧/④
PL-23	152.7	476.2	320.2	116.7	78.5	-	259.6	96.1	0.59	-	0.50	0.84
C-23	134.1	425.4	443.0	323.4	88.3	-	-	343.4	0.66	-	-	1.06
C-4	134.7	425.3	452.3	519.6	98.1	421.8	476.2	-	0.73	0.99	1.05	-
C-23-Pcc	126.6	198.5	211.4	323.4	98.1	196.2	245.3	-	0.77	0.99	1.16	-
C-4-ENC	135.7	195.3	225.6	519.6	117.7	186.4	211.4	-	0.57	0.95	0.94	-
C-4-REB	136.4	273.4	302.2	467.4	98.1	264.9	323.7	-	0.72	0.97	1.07	-

P_{cr}: cracking load, P_y: yield load, P_u: ultimate load, P_{ab}: shear buckling load; NOTE: Subscript denotes measured value

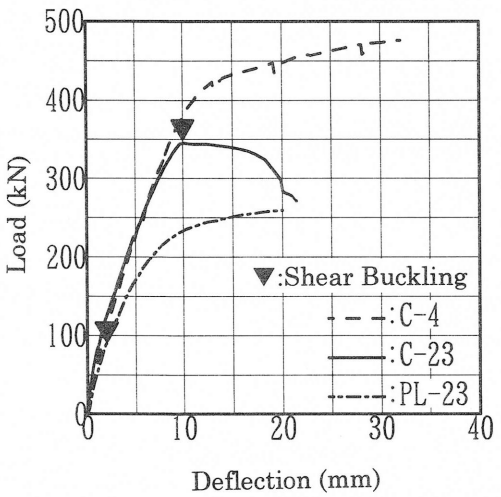

Fig. 13. Load-Deflection Relationship

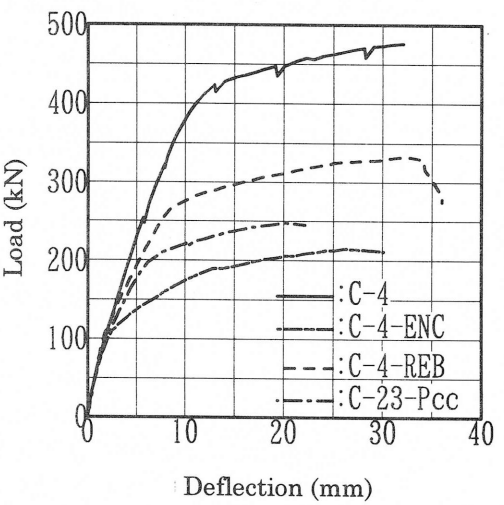

Fig. 14. Load-Deflection Relationship

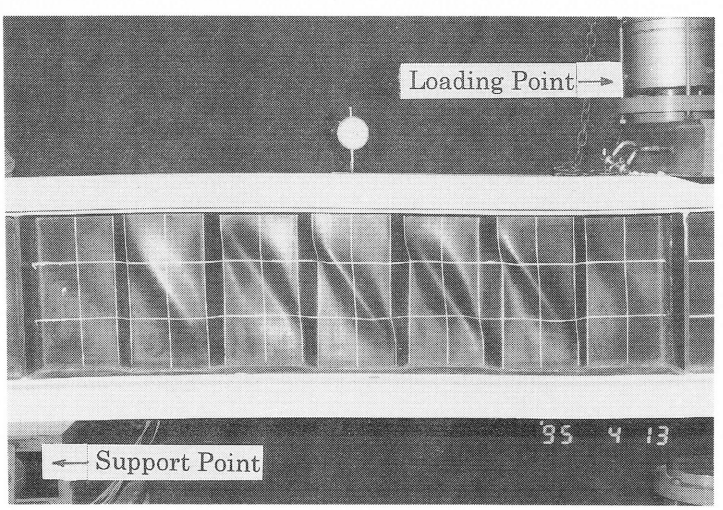

Phote.2 Shear Buckling of Corrugated Web

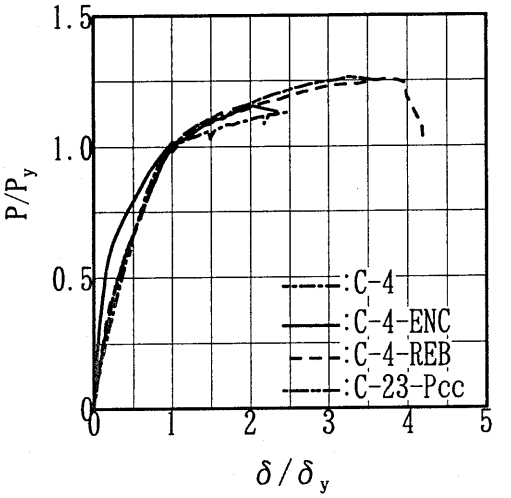

Fig. 15. Normalized Load-Deflection Relationship

The load-deflection relationships for specimens C-23-Pcc, C-4-ENC, and C-4-REB are shown in Fig. 14. The relationship for the standard test specimen C-4 is shown for reference. In the case of specimen C-4-ENC, for which specimen C-4 is the standard and the load standard is at the load was 178kN level (P/P_y=0.42), at the load of 79kN, there was slippage and separation observed at the interface between the corrugated steel web and the lower concrete flange. Also, for the standard specimen C-4 with a load level of 400kN (P/P_y=0.95), at the load of 177kN, there was a local failure seen to occur in the front face of the diagonal panel in the joint between corrugated web and lower concrete flange. At a deflection of 26mm, corresponding to $2\delta_y$, diagonal failure occurred in the bottom concrete flange and the maximum load-bearing capacity was exhibited under this condition. However, the structural integrity of the girder was confirmed even with the occurrence of slippage and separation components, and it was confirmed that the local bearing failure occurred in the lower concrete flange and the integrity of the girder was maintained even to its ultimate stage. Also, for specimens C-23-Pcc, C-4, and C-4-ENC, loading test was terminated at the 2~3 δ_y stage after yield of the PC tendons.

In specimen C-4-REB, no slippage and separation at the connection between the corrugated steel web and the bottom concrete flange was noted, and noise related to slipping, which was audible with specimen C-4-ENC, could not be heard. The distribution of normal strain in the longitudinal direction of the connecting rebars showed the same pattern as that in the longitudinal reinforcement, and it indicated the same bond strength as the longitudinal reinforcement. Thus, it was confirmed that the integrity of the girder was maintained due to the shape of the corrugation and the connecting rebars. The ultimate load of specimen C-4-REB was 1.5 times larger than that of specimen C-4-ENC which had no connecting rebars, so the connecting rebars are shown to contribute to flexural strength. In the ultimate stage of specimen C-4-REB, the girder failed by tensile rupture of the PC tendons in the bottom concrete flange.

Fig. 15 is a normalized expression of Fig.14 divided by P_y and δ_y, where P_y and δ_y are the yield load and yield displacement, respectively. The normalized relationship shows good agreement among the three specimens, with the exception of Specimen C-4-ENC, and it is confirmed that the flexural shear behavior is similar. For Specimen C-4-ENC, there was slippage at the connection between concrete and steel web from the initial stage of the loading test, and the differences in deflection can be attributed to this. Also, the maximum load-bearing capacity was seen at 3~4 δ_y loading, indicating that the ductility ratio was about the same for each specimen.

In Specimen C-23-Pcc, where the steel flange was not continuous in the precast structure with the corrugated steel web, the normalized load-deflection relationship shows good agreement with specimen C-4, and it is confirmed that the load-carrying characteristics are similar to those of normal girders. Also, for specimen C-4-REB where the girder with the connecting rebars was welded to the lower edge of the corrugated steel web and embedded in the concrete, the normalized load-deflection relationship is in good agreement with that of specimen C-4. These results indicated that shear connection using this connecting rebar maintains composite action as well as studs, and it is confirmed that girders with connecting rebars as shear connectors have excellent loading characteristics.

5.3.2 DISTRIBUTION OF NORMAL STRAIN

The distribution of normal strain for specimens C-4, C-23-Pcc, and C-4-REB is shown in Fig. 16. It is clear that there was almost no strain created in the web of the composite PC girders with corrugated steel webs when the prestressing force was initially applied, and the prestressing force was transferred effectively to the concrete flange. When the static load was applied in the loading test, until yielding of the main tensile steel member there was no normal strain created in the corrugated steel web, and it is confirmed that the corrugated steel web was unable to resist the

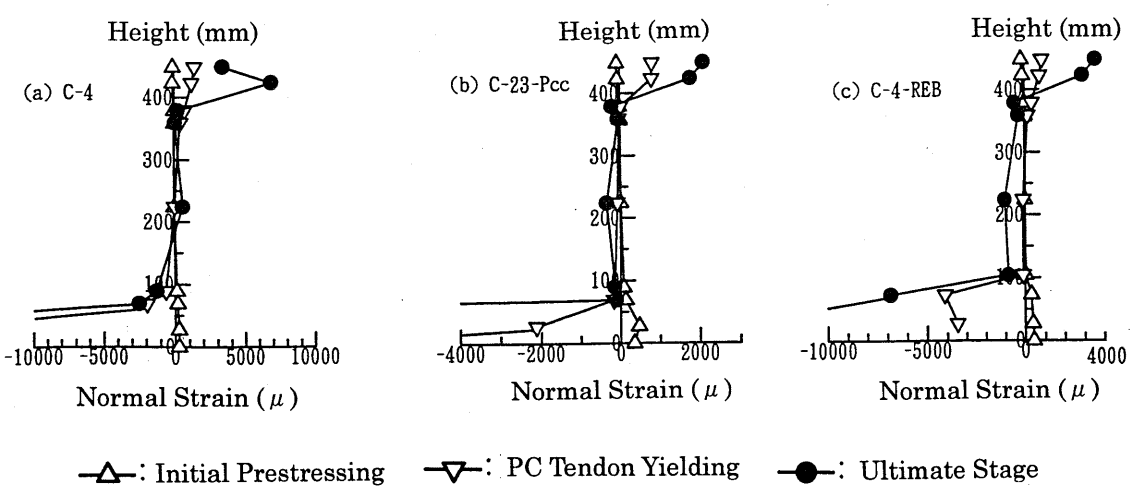

Fig. 16. Normal Strain Distribution

bending moment. However, in specimen C-4, after yielding of the lower steel flange, which is the main tensile steel member, normal strain reading maximum of 600μ was seen in the corrugated steel web, and for specimens C-4-ENC and C-4-REB, after yielding of the PC tendon, which is the main tensile steel member, normal strain was seen in the corrugated steel web to a maximum order of 1000μ. This then indicates that when the main tensile steel member yields, a corrugated steel web will resist the bending moment. In specimen C-23-Pcc, no normal strain was seen in the steel flange at the center of the span where the maximum bending moment occurred in the steel flange, indicating that the steel flange could not resist the bending moment. Therefore, it was indicated that the steel girder portion of C-23-Pcc resisted only the shear forces.

When composite structures using corrugated steel webs reach the serviceability limit state, variations in normal strain are small in the steel portions and at welds in the connecting rebars. The stress reaches only 30MPa, and so fatigue strength of the steel portion and the welded portion of the connecting rebars can be considered negligible.

5.3.3 RESULTS OF ANALYSIS OF DEFLECTION

The calculated and measured values of the load-deflection relationships for the PC Series are shown in Fig. 17 and Fig. 18. The calculated value is obtained by fiber model analysis described in Chapter 4. For specimen C-23, until shear buckling occurs in the web, the calculated value and measured value are in good agreement. For specimens C-23-Pcc, C-4, C-4-ENC, and C-4-REB, the calculated values for initial flexural stiffness, flexural stiffness after cracking, and yield load of the PC tendon are all in good agreement with the measured values. Hence, it is considered feasible to calculate the amount of deflection of composite PC girders with corrugated steel plates based on the assumptions made in the calculation method in Chapter 4.

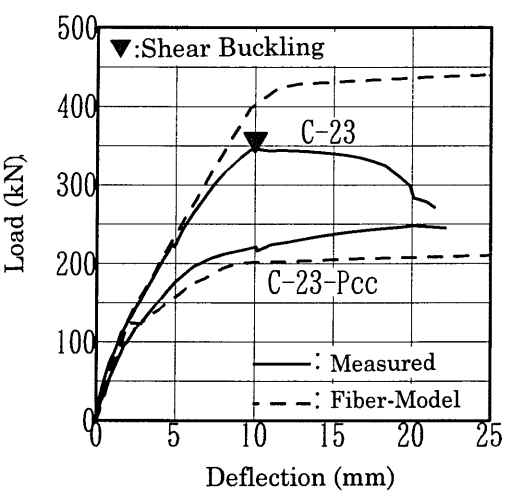

Fig. 17. Calculated Value and Measured Value of Load-Deflection Relationship (C-23,C-23-Pcc)

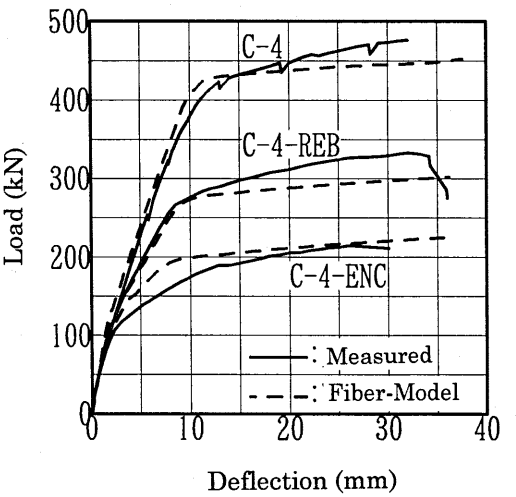

Fig. 18. Calculated Value and Measured Value of
Load-Deflection Relationship (C-4,C-4-ENC,C-4-REB)

5.3.4 STUDY OF INTERACTION

(1) THE INTERACTION MECHANISM

The basic mechanism of interaction in the proposed new type of shear connector, in which a corrugated steel web is embedded into the concrete, will be investigated for specimen C-4-ENC. In this specimen, when there is slippage and separation between the corrugated steel web and the lower concrete flange at the point where the two materials meet, it was observed that a gap opens up on one side of the corrugated steel plate in the concrete flange as shown in Photo.3. In this study, it was decided to assume that apparent friction in the interaction mechanism occurred as a result of bonding. The interaction mechanism between the perpendicular face of the diagonal panel and the concrete will be investigated as shown in Fig.19, where the sum of forces can be separated into Force N (transversel force) and Force T (longitudinal force). Hence the apparent friction coefficient μ^* between the corrugated steel plate and the concrete can be represented by Eq. (7) as follows.

$$\mu^* = \tan\left(\tan^{-1}\mu + \theta\right) \tag{7}$$

where:

μ^*: apparent friction coefficient between corrugated steel plate and concrete
μ : friction coefficient between steel plate and concrete
θ : fold angle of the corrugated steel plate

The relation between apparent friction coefficient μ^* calculated from Eq. (7), and friction coefficient μ is shown in Fig. 20. For the corrugated steel plate, as the fold angle θ increases, the apparent friction coefficient also increases, and it can be confirmed that the frictional action is greater than for a flat steel plate ($\theta = 0°$). For the corrugated steel plate used in this study ($\theta = 53.13°$) assuming the friction coefficient μ between steel plate and concrete as 0.65 from previous studies, then it can be seen that the apparent friction coefficient μ^* will be about 20 [20][21]. From experimental results for specimen C-4-ENC, transversel force N is calculated from the hoop reinforcement at the center of the shear span and the horizontal shear force T (longitudinal force) is calculated using the vertical shear force, and then the relationship between the apparent friction coefficient μ^* and transversel force N is as shown in Fig. 21. In the section A~B in this figure, there is an almost linear relationship between apparent friction coefficient μ^* and transversel force N, and the maximum value of the friction coefficient μ is about 0.68. The maximum apparent friction coefficient μ^* is about 21, which is in very close agreement with the calculated value given by Eq.(7), and this confirms that integration of the corrugated steel plate and concrete is valid. In section B~C of the same figure, with the decline in apparent friction coefficient μ^* there is a sudden increase in transversel force N, and indicating that there is a shift between the corrugated steel plate and the concrete flange. However, even when local failure of the bearing with the lower concrete flange occurs in the ultimate stage of the loading test, the apparent friction coefficient μ^* between the corrugated steel plate and concrete is about 3.5, indicating that the integrity of the composite girder remains sound.

(2) ULTIMATE STRENGTH OF SHEAR CONNECTOR

The ultimate shear strength provided by a corrugated steel web embedded in a concrete flange, with the diagonal panel of the corrugated steel web as the block connector as shown in Photo.3 and the connecting rebar as the reinforcement of the shear connector, is given by Eq.(8) [22]. The first term an the right-hand side of Eq.(8) represents the horizontal shear forces that one diagonal panel of the corrugated steel web can withstand, and the second term indicates the horizontal shear force that the connecting rebar can withstand. In this equation, in the yield condition, the connecting rebar responds with yield stress and the concrete responds with $(3/5)f'_{ck}$.

$$Q_u = \frac{3}{5} f'_{ck} A_1 + \sigma_{sy} A_2 \qquad (8)$$

where:

Q_u : ultimate strength of shear connector
f_{ck} : compressive strength of concrete
σ_{wy} : yield strength of connecting rebar
A_1 : area of embedded panel
A_2 : cross-sectional area of connecting rebar

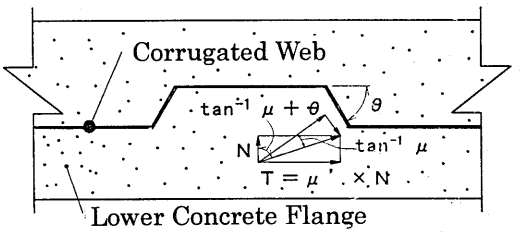

Fig. 19. Interaction Mechanism for Corrugated Steel Web and Concrete

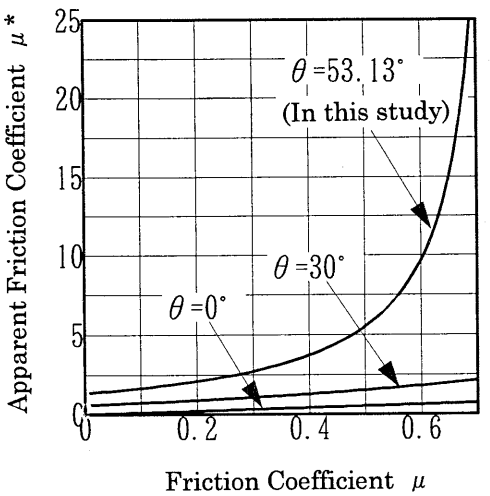

Fig. 20. $\mu - \mu^*$ Relationship

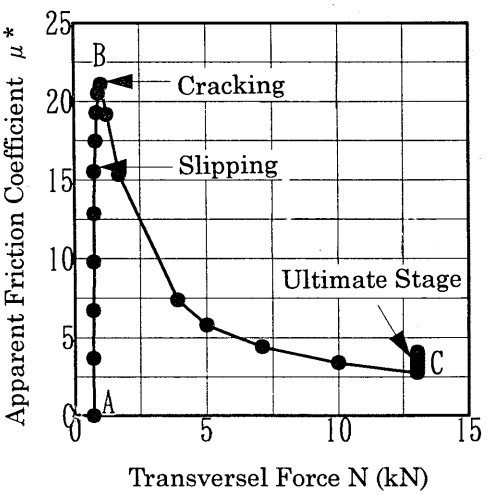

Fig. 21. Apparent Friction Coefficient μ*

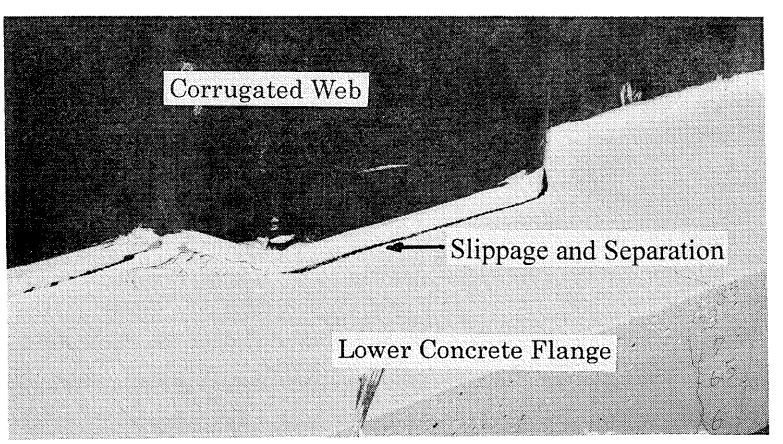

Photo.3 Slippage and Separation between Corrugated Steel Web and Concrete

The calculated value given by Eq.(8) and the horizontal shear force at local bearing failure in the concrete are shown in Table 7.

The horizontal shear force at local bearing failure was obtained from an elastic calculation in which the concrete was included in the cross section of the girder by use of the vertical shear force obtained from the applied load.

The horizontal shear force at local bearing failure in the concrete for specimen C-4-ENC was 177 kN; the calculated value given by Eq.(8) is in very close agreement. Also, from the results of the calculation, the ultimate strength of the shear connector in specimen C-4-REB is five times better than that in C-4-ENC, thus confirming that the connecting rebar is very effective as a shear connector.

Table. 7 Ultimate Strength of Shear Connector

(Unit: kN)

Specimen	Value of Eq.(8)	Horizontal Shear Force
C-4-ENC	44.6	43.4 [1)]
C-4-REB	215.4	---

1)Local failure of bearing occurs

6. CONCLUSIONS

Flexural shear tests were conducted on girders with corrugated steel webs together composite PC girders with corrugated steel webs. Further, relatively simple equations are proposed for calculating the shear buckling strength of corrugated steel plates. Three modes of buckling for the corrugated steel plates are considered in an unified manner. The results of the study lead to the following conclusions:

(1) The proposed equations for the shear buckling strength give good agreement with the experimental results.
(2) It is shown that corrugated steel plates as webs give a shear buckling strength is three times greater than flat plates. However, for girders with corrugated steel webs, when shear buckling occurs in the web, there is rapid loss in strength. It is thus not wise to depend on post-buckling strength, and the behavior of corrugated web girders cannot be considered the same as that of normal plate girders.
(3) The out-of-plane rigidity of corrugated steel webs is larger than that of flat steel webs, so it is possible to eliminate the longitudinal stiffener except at support points and where loads are concentrated.

(4) Corrugated steel webs display no resistance to bending moment, and they only counteract shear stress. It has been shown that corrugated steel webs become an almost pure shear stress field.
(5) By using girders with corrugated steel webs in composite PC structures, it will be possible to make good use of structures with shear strength, especially those with large shear buckling strength of the corrugated steel web.
(6) Composite PC girders where the steel flange is not continuous in the precast structure with the corrugated steel web are shown to have similar load-bearing characteristics to those of normal girders.
(7) The integrity of composite girders with corrugated steel webs can be ensured by embedding the corrugated steel web in the lower concrete flange, and integrity can be further enhanced by installing a slip prevention mechanism.
(8) With a deformed reinforcing bar welded to the lower edge of the corrugated steel web, the lower edge of the web is embedded into the bottom concrete flange as a unitized structure. There is almost no visible cracking between web and concrete flange where the two materials come together, and it has been shown that the girder acts as a single unit. The requirements of mechanical behavior and serviceability state are satisfied.

Acknowledgements

We are greatly indebted to P.S. Corp. and NKK Light Steel Corp., as well as to technical engineer Mr. Yutaka Morishita of the Yokohama National University and to Mr. Jun Tajima of Taisei Corp., all of whom rendered valuable assistance in performing the experiments. This study was partly supported by Grant-in-Aid for Scientific Research from the Ministry of Education, Science and Culture of Japan (B(2) No.07555141, Principal Investigator: Prof. Shoji Ikeda, Yokohama National University)

References

[1] Ikeda, S.: Hybrid Structures in Civil Engineering Construction, Journal of Prestressed Concrete, Vol.37 No.2, pp.16-19, Mar 1995 (in Japanese)
[2] J. Combault: The Maupre Viaduct Near Charolles, AISC National Steel Construction Conference, Feb 1988
[3] J. Combault, et al: Box-Girders Using Corrugated Steel Webs and Balanced Cantilever Construction, FIP Symposium Kyoto, pp.417-424, Oct 1993
[4] Kondo, M., Simizu, Y., Ohura, T., and Hattori, M.: Prestressed Concrete Bridge Using Corrugated Steel Webs –Sinkai Bridge, Journal of Prestressed Concrete, Vol.37 No.2, pp.69-78, Mar 1995 (in Japanese)
[5] Simada, S: Shear Strength of Steel Plate Girders with Folded Web Plate (Ripple Web Girder), Proceedings of JSCE,No.124, pp.1-10, Dec 1965 (in Japanese)

[6] Tagawa, K., and Okamoto, H.: Study on the Corrugated Folded Plate as Earthquake Shear Wall (Part 1, Folded Corrugated Plate), Summaries of Technical Papers Annual Meeting of AIJ (Hokuriku), pp.1093-1094, Oct. 1974 (in Japanese)

[7] Kawada, K., Okamoto, H., and Tanaka, K: Studies on Corrugated Web Girders , NKK Technical Report, No.71, pp.25-33,Oct. 1976 (in Japanese)

[8] Yamaguchi, K., Yamaguchi, T., and Ikeda, S.: Flexural Shear Behavior of Corrugated Steel Web Structures, Proceeding of The 3rd Symposium on Research and Application of Composite Constructions, pp.77-82, Nov.1995 (in Japanese)

[9] Yamaguchi, K., Yamaguchi, T., and Ikeda, S.: Flexural Shear Behavior of Composite Prestressed Concrete Structures with Corrugated Steel Webs, Proceeding of The 5th Symposium of Developments in Prestressed Concrete, pp.339-344, Oct.1995 (in Japanese)

[10] Tajima, J., Yamaguchi, K., and Yamaguchi, T.: Study on Shear Buckling Characteristics on Composite Structures with Corrugated Steel Web, Proceeding of the 50th Annual Conference of JSCE, pp.94-95, Sept. 1995 (in Japanese)

[11] Yamaguchi, K., Yamaguchi, T., and Ikeda, S.: The Shear Buckling Behavior of Composite Structures with Corrugated Steel Webs, Proceeding of The 4th Symposium of Developments in Prestressed Concrete, pp.235-240, Oct.1994 (in Japanese)

[12] Hasegawa, A., Nishino, F., and Okumura, T.: Ultimate Strength of the Longitudinally Stiffened Plate Girders in Shear, Proceedings of JSCE, No.235, pp.13-28, Mar. 1975 (in Japanese)

[13] JSCE, "Guidelines for Stability Design Steel Structures," Oct. 1987 (in Japanese)

[14] J. T. Easley: Buckling Formulas for Corrugated Metal Shear Diaphragms, ASCE ST.7, pp.1403-1417, July 1975

[15] Wolchuk, R., and Mayrbaurl, R.M.: Proposed Design Specifications for Steel Box Girder Bridges, Report No. FHWA-TS-80-205, U. S. Department of Transportation, Federal Highway Administration, Office of Research and Development, Washington, D. C., Jan. 1980

[16] J. Lindner, und R. Aschinger: Grenzschubtragfähigkeit von I-Trägern mit trapezförming profilierten Stegen, Stahlbau Nr. 57 H.12, pp.377-380, 1988

[17] Hanada, T., Kato, S., Takahashi, K., and Yamazaki, M. : Model Experiment of Continuous PC Box Girder with Corrugated Steel Web (MatsunikiNo.7Bridge), Proceeding of The 5th Symposium of Developments in Prestressed Concrete, pp.345-350, Oct.1995 (in Japanese)

[18] K. Basler: Strength of Plate Girder in Shear, ASCE Vol. 87, ST7, pp.150-180, Oct. 1961

[19] Fujii, T.: On an Improved Theory for Dr. Basler's Theory, Final Report of 8th Congress of IABSE, New York, pp.479-487, Oct. 1968

[20] Sato. M., and Ishiwata, M.: Bond Characteristics between Concrete, Flat and Lugged Steel Plate, Proceedings of JCI, Vol.2, pp.365-368, 1980 (in Japanese)

[21] Sonoda, K., Kitoh, and H., Nakajima, K.: An Experimental Study on the Bond Characteristics of Embossed Steel Plates, Proceeding of The 3rd Symposium on Research and Application of Composite Constructions, pp.155-160, Nov.1995 (in Japanese)

[22] Japan Road Association, "Specification for Highway Bridges, Part II," pp.256-259, Feb. 1973 (in Japanese)